İstanbul Yerbilimleri Dergisi, C.27, S.2, SS. 59-76, Y. 2014

8 OCAK 2013 (M_w=5.7) VE 24 MAYIS 2014 (M_w=6.8) KUZEY EGE DEPREMLERİNİN KAYNAK ÖZELLİKLERİ VE ONLARIN ARTÇIŞOKLARI

SOURCE CHARACTERISTICS OF THE JANUARY 8, 2013 (M_W=5.7) AND MAY 24, 2014 (M_W=6.8) NORTH AEGEAN EARTHQUAKES AND THEIR AFTERSHOCKS

Doğan Kalafat [1], Kıvanç Kekovalı [1], Ali Pınar [2]

[1] Boğaziçi University Kandilli Observatory & Earthquake Research Institute, National Earthquake Monitoring Center, 34684, Çengelköy-İstanbul

[2] Boğaziçi University Kandilli Observatory & Earthquake Research Institute Earthquake Engineering Department,34684, Çengelköy- İstanbul

Yayına Geliş(Received): 16.02.2016, Yayına Kabul (Accepted):10.04.2016, Basım (Published): Şubat/February 2017 Corresponding Autor: Doğan Kalafat
e-mail: kalafato@boun.edu.tr

Öz

Kuzey Ege Denizi, Avrasya ve Afrika tektonik plakalar arasındaki en önemli aktif sismik ve deformasyon alanlarından birisidir. 8 Ocak 2013 tarihinde 14:16 UTC (16:16 yerel saat ile) orta büyüklükte bir deprem (Mw= 5.7) meydana gelmiştir. Deprem, Gökçeada'nın güneyi ve Bozcaada adasının güneybatısı arasında meydana gelmiştir. Deprem geniş bir alanda hissedilmiş olup, özellikle kuzeydoğu Yunanistan Limni Adasının güneyinde, kuzeybatı Türkiye ve çevresinde, örneğin Çanakkale, Marmara Bölgesi ve Kuzey Ege kıyılarından Atina ya kadar hissedilmiştir. Dış merkez koordinatlarının 39.669°N-25.533°E olarak hesaplanmıştır ve odak derinliği Kandilli Rasathanesi ve Deprem Araştırma Enstitüsü (KRDAE) tarafından 13.1 km olarak hesaplanmıştır. Ana şoktan sonraki ilk 40 saat içinde büyüklükleri Ml=1.6-5.0 olan 160 artçı sarsıntı meydana gelmiştir. Bölge, Kuzey Anadolu Fayı'nın (KAF) kuzey kolunun Ege Denizi içindeki devamı olarak tanımlanmaktadır. Bu çalışmada belirlenen fay düzlemi çözümleri, depremin KD-GB yönelimli doğrultu atımlı fay segmenti üzerinde meydana geldiğini göstermektedir. Keza Artçı depremlerin dağılımı da kırılmanın KD-GB yönelimli fay segmentinde meydana geldiğini desteklemektedir.

Diğer bir büyük deprem yaklaşık 17 ay sonra aynı bölgede meydana gelmiştir. 24 Mayıs 2014'te 09:25 UTC de (00:25 yerel saat), çok şiddetli bir deprem Ml=6.7 (Mw=6.8) meydana gelmiştir. Deprem özellikle Yunanistan ve Türkiye etkili olmuş olup, dış merkezi Çanakkale'nin 87 km batısındadır, ve deprem sonucu 350 kişi Yunanistan ve Türkiye'de yaralanmıştır. Deprem Yunanistan, Türkiye, Bulgaristan ve Romanya'da kuvvetli hissedilmiştir. Ana şoktan sonraki ilk 96 saat içinde büyüklükleri M=0.9- 4.8 olan 576 artçı sarsıntının çözümü yapılmıştır. Ana şok meydana geldikten sonra açığa çıkan enerjinin büyük bir bölümü KD-GB doğrultulu fay parçasında serbest bırakılmıştır (yönelme etkisi). Bu nedenle deprem Çanakkale, İstanbul ve Marmara bölgesinde kuvvetli hissedilmiştir. Bu çalışmada toplam 50 depremin, ana şok ve önemli artçı şokların (M> 4.0) moment tensor CMT çözümleri yapılmıştır. Moment tensör çözümleri genellikle doğrultu atımlı faylanma göstermektedir. Depreme sebep olan fayın, Kuzey Anadolu Fay Zonu'nun Kuzey Ege Denizi'nden geçen bir kolu üzerinde olduğu düşünülmektedir. Genellikle, depremlerin lokasyonu,KD-GB düğüm düzlemleri, Kuzey Ege Çukurluğu (NAT) içinde sağ yanal faylanma ile tutarlıdır. Ege Denizi, Kuzey Ege çukurluğuna (NAT) paralel KD-GB doğrultulu sağ yönlü doğrultu atımlı faylanmalar boyunca ile karakterize edilir. Bu Doğrultu atımlı faylanma karakteri, özellikle Ege kıyılarından KD ve Batı Türkiye kıyılarına oblik faylara dönüşürek uzanmaktadır. Gerilme analizi sonuçları, bölgedeki hakim Pmax-sıkışma ekseninin **BKB-DGD** yönünde ve Tmax-genişleme ekseninin de **KKD-GGB** yönünde olduğunu göstermektedir.

Anahtar Kelimeler: Kuzey Ege Bölgesi, depremsellik, aktif faylanma, artçışok, CMT çözümü

Abstract

The North Aegean Sea is one of the most seismically active and deforming regions between the Eurasian and African tectonic plates. On 8th January 2013 at 14:16 UTC (16:16 local time) a moderate earthquake (Mw= 5.7) occurred between the south of Gökçeada and southwest of Bozcaada Islands. The earthquake was felt in a wide area. It was especially felt in the NE Greece south of Lemnos Island, NW Turkey and surrounding areas, such as Çanakkale, Marmara Region and Northern Aegean coast as well as in Athens. The epicentral coordinates were calculated as 39.669°N-25.533°E and the focal depth was 13.1 km according to the Kandilli Observatory & Earthquake Research Institute (KOERI). After the main shock, 160 aftershocks occurred with magnitudes Ml=1.6-5.0 within the first 40 hours. The area is defined as the continuation of the northern branch of North Anatolian Fault (NAF) inside the Aegean Sea. The fault plane solution determined in this study shows that the earthquake occurred on a NE-SW oriented strike slip fault segment. The aftershock distribution also supported the rupture of the NE-SW oriented fault.

Another big earthquake occurred in the same area approximately 17 months later. On 24th May 2014, at 09:25 UTC (12:25 local time), a powerful Ml=6.7 (Mw=6.8) earthquake hit Greece and Turkey, 87 km west of Çanakkale, and 350 people were injured in Greece and Turkey. This earthquake was strongly felt in Greece, Turkey, Bulgaria and Romania. After this earthquake, 576 aftershocks were determined with magnitude range M=0.9- 4.8 in the first 96 hours. The main-shock occurred on a fault with a NE-SW strike where the largest portion of the energy was released towards these directions (directivity effect). Therefore the earthquake was felt strongly in Çanakkale, Istanbul and Marmara region. In this study we calculated Centroid Moment Tensor CMT solutions for the main-shock and important aftershocks (M>4.0). CMT analyses were done for 50 important earthquakes. Moment tensor solutions generally indicate strike-slip faulting. The fault which caused earthquake, is thought to be a branch of the North Anatolian Fault Zone in the North Aegean Sea. Generally, the location of the earthquakes and orientation of the NE-SW nodal planes are consistent with right-lateral faulting within the North Aegean Trough (NAT). The Aegean Sea is characterized by dextral strike-slip faulting along NE-SW striking faults that are formed parallel to the North Aegean Trough (NAT). The strike-slip faulting changes to oblique-slip faulting, with significant component of extension, as one goes from the Aegean to the coastal area of NE and Western Turkey. The results of the stress analysis show that the (**P**-compressional) direction of the stress axes is in **WNW-ESE** direction and (**Tmax**-extensional) direction is in **NNE-SSW** direction.

Keywords: North Aegean Region, seismicity, active faulting, aftershock, CMT solution

INTRODUCTION

The Aegean Sea, is one of the most seismically active areas of the Eastern Mediterranean region (Figure 1). Generally, North Aegean Sea region has been tectonically developed after the collision of Arabian plate with the Eurasian in the Late Miocene time and the subsequent westward escape of the Anatolian Plate relative to the Eurasian Plate, during the Early Pliocene (McKenzie, 1978; McKenzie and Jackson, 1983, Taymaz et al. 1991; Barka, 1992; Barka and Gülen 1988; Papazachos et al., 2000; Tranos, 2009; Kiratzi and Svikkas, 2013). The North Anatolia Fault Zone (NAFZ) accommodates much of the right-lateral, strike-slip motion between the Anatolian Block and the Eurasia Plate (Allen, 1969; McKenzie, 1972; Dewey, 1976; Dewey and Şengör, 1979; Jackson ve McKenzie, 1984; Şengör et al., 1985; Barka et al., 1987).

NAFZ is one of the most active and important fault zones in the world. Especially, faults within the North Aegean Trough (NAT) represent the northern branch of the North Anatolian Fault Zone (NAFZ), the major transform faulting structure in northern Turkey accommodating the westward motion of the Anatolian plate with respect to Eurasia, at a rate of approximately 25 mm/yr (Reilinger et al.,1997; Papazachos,1999; McClusky et al., 2000).

The NAT corresponds to an approximately 300 km long system of tectonically active marine basins, representing the extension of the North Anatolian Fault Zone (NAFZ) into the Aegean Sea ([Le Pichon et al., 1987.; Kreemer et al., 2004). The study area is dominated by dextral strike-slip faulting and is characterized by frequently occurring strong earthquakes (Figure 1).

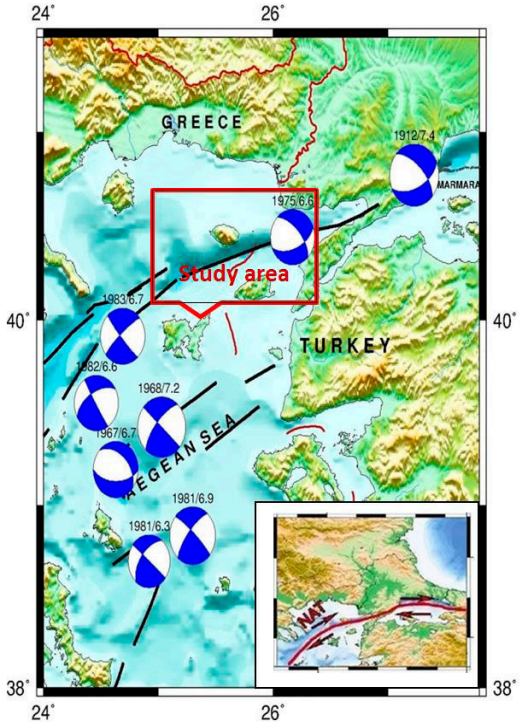

Figure 1. Active faults in the study area and faulting mechanisms of major earthquakes in the last century. (faults are taken from Saroglu et al., 1992, MTA; NAT North Aegean Trough)
Şekil 1. Çalışma bölgesindeki aktif faylar ve son yüzyılda meydana gelmiş büyük depremlerin faylanma mekanizmaları (Faylar Saroglu ve diğ., 1992, MTA; Kuzey Ege Çukuru)

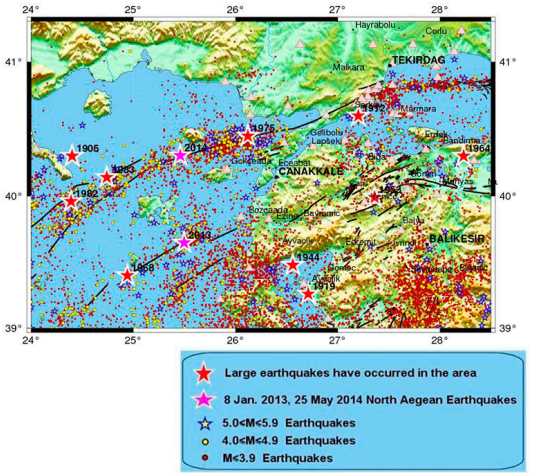

Figure 2. Strong earthquakes, recent seismicity, active faults in the region and the triangles show the seismic stations in the region from Turkish and Greece Seismological Networks.
Şekil 2. Büyük depremler, güncel depremsellik, bölgedeki aktif faylar ve üçgenler Türk ve Yunan sismik ağlarına ait bölgedeki deprem istasyonlarını göstermektedir.

Table 1. Important Earthquakes in the region (1900-2014)

Eq.No.	Date	O. Time	Latitude	Longitude	Depth	Ms	Location
1	08.11.1905	22:06:00.00	40.30	24.40	14.0	7.4	GREECE
2	09.08.1912	01:29:00.00	40.60	27.20	16.0	7.3	MUREFTE-SARKOY (TEKİRDAG)
3	10.08.1912	09:23:00.00	40.60	27.10	15.0	6.3	MUREFTE-SARKOY (TEKİRDAG)
4	20.08.1917	23:02:09.60	40.30	25.43	40.0	6.0	AEGEAN SEA
5	18.11.1919	21:54:50.30	39.26	26.71	10.0	7.0	KUCUKKOY-AYVALIK (BALIKESİR)
6	04.01.1935	14:41:30.40	40.40	27.49	30.0	6.4	GULF OF ERDEK (MARMARA SEA)
7	04.01.1935	16:20:04.60	40.30	27.45	20.0	6.3	GUVEMALANI-BIGA (ÇANAKKALE)
8	22.09.1939	00:36:36.60	39.07	26.94	10.0	6.6	DIKILI-BERGAMA (İZMİR)
9	28.10.1942	02:22:53.10	39.10	27.80	50.0	6.0	KARAKURT-KIRKAGAC (MANİSA)
10	06.10.1944	02:34:48.70	39.48	26.56	40.0	6.8	GULF OF EDREMİT (EGE DENİZİ)
11	18.03.1953	19:06:16.10	39.99	27.36	10.0	7.2	YENICE-GÖNEN (ÇANAKKALE)
12	06.10.1964	14:31:23.00	40.30	28.23	34.0	7.0	MANYAS-KARACABEY (BURSA)
13	04.03.1967	17:58:09.00	39.25	24.60	60.0	6.5	AEGEAN SEA
14	19.02.1968	22:45:42.40	39.40	24.94	7.0	7.1	AEGEAN SEA
15	27.03.1975	05:15:07.90	40.45	26.12	15.0	5.7	GULF OF SAROS (AEGEAN SEA)
16	19.12.1981	14:10:51.10	39.22	25.25	10.0	7.2	AEGEAN SEA
17	18.01.1982	19:27:25.00	39.96	24.39	10.0	6.9	GREECE
18	18.01.1982	19:31:07.90	40.03	24.56	10.0	5.4	AEGEAN SEA
19	06.08.1983	15:43:51.90	40.14	24.75	2.0	6.9	AEGEAN SEA
20	08.01.2013	14:16:07.19	39.65	25.50	8.0	5.8	AEGEAN SEA
21	24.05.2014	09:25:01.59	40.30	25.46	21.2	6.9	AEGEAN SEA

For example, during the last century many destructive earthquakes occurred in this region (Figure 2; Table 1). The 1905 Greece (Io=IX; many casualties, M=7.5), 1912 Saros-Mürefte-Şarköy (Io=X; 2836 casualties; Ms=7.4), 1919 Soma-Ayvalık (Io=IX; many casualties; Ms=6.9), 1968 North Aegean Sea (Io=IX; 20 casualties; Ms=7.1), 1975 Gulf of Saros (Io=VII; Ms=6.6), 1982 (M=7.0), 1983 (M=6.8) are the most important earthquakes in the region (Drakopoulos and Ekonomides, 1972; Eyidoğan et al., 1991; Papazachos et al., 1998; Papadimitriou and Sykes, 2001; Vannucci and Gasperini, 2004; Kalafat et al., 2011).

On 8th January 2013 at 14:16 UTC (16:16 local time) a moderate earthquake (Mw= 5.7) occurred between the south of Gökçeada and southwest of Bozcaada Islands. On 24th May 2014, at 09:25 UTC (12:25 local time), a powerful Ml=6.7 (Mw=6.8) earthquake occurred 87 km west of Çanakkale in the Agean Sea.

This study covers seismicty, aftershock distribution, moment tensor inversion for important aftershocks of 2013-2014 sequences. This is important in order to understand more accurate tectonic regime of the study region. Also we calculated stress tensor inversion, b values for 2013-2014 North Aegean Sea Earthquakes. We found source features of the May 24, 2014 North Aegean Earthquake. According to

the our solution the source rupture area extends. The direct relationship wasn't found between the 2014 earthquake and the NAFZ by Saltogianni et al., 2015

Also we found long period pulses associated with the 2014 North Aegean earthquake recorded at Gökçeada strong motion station. We have applied teleseismic bodywave modelling for 2014 Earthquake. In addition, we investigated Coulomb Stress Changes in this area in order to asses areas of subsequent off fault aftershocks.

2014 North Agean Sea Earthquakes have studied using the seismological and geodetic inversions of teleseismic waveforms by Saltogianni et al., 2015. They found that the faulting of the earthquake shows shallow strike slip, likely to a fault consisting of two segments.

DATA AND METHODOLOGY

The Turkish and Greek seismic networks

The 2013 and the 2014 North Aegean Earthquake sequences were recorded by the stations of the Turkish and Greek Seismological Networks (Figure 2). The Turkish seismic stations are located to the east of the source regions of both the earthquakes resulting in large seismic gap. Similarly, the Greek stations are located mostly to the west of the source regions. For this reason, we need to merge data from the Turkish and Greek seismic stations to provide better station coverage for the location of the mainshock and also for the aftershocks. Moreover, a good azimuthal coverage is essential for CMT solution algorithms we applied. Generally, both the networks are equiped with broadband and strong motion sensors such as Guralp CMG 3T, CMG 5TD, CMG-3ESP.

For the location of the aftershocks we used HYPO71 (Lee and Lahr, 1975) and HYPOINV (Klein, 2002) to obtain initial locations. For the locations we used 1-D local crustal and velocity model (Figure 3; Kalafat et al., 1983) and Vp/Vs ratio of 1.73 which we calculated from our database using the Wadati technique.

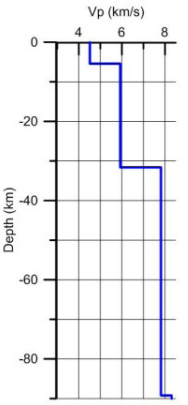

Figure 3. 1-D velocity © xmodel used to locate the earthquakes of Aegean Sea.
Şekil 3. Ege Denizi depremlerinin lokasyonunda kullanılan 1 boyutlu hız modeli.

SOURCE FEATURES OF THE MAY 24, 2014 NORTH AEGEAN EARTHQUAKE

The source rupture area extent

The most prominent feature of the earthquake is the widespread distribution of the aftershocks. The routine fast locations carried out by the National Earthquake Monitoring Center (NEMC) of KOERI portreys a lateral variation of longitudes between 25.0°E and 26.2°E. This corresponds to approximately 120 km fault rupture length if all the aftershocks take place along the ruptured fault plane. Using the USGS estimated seismic moment magnitude of Mw=6.9 and the relation between fault rupture length and moment magnitude of Wells and Coppersmith(1994),(Log(L) =(Mw-5.16±0.13)/1.12±0.08) yields a rupture length between 35-60 km. Thus estimated rupture lenght is a few times shorter than the rupture derived from the aftershok distribution (Figure 4).

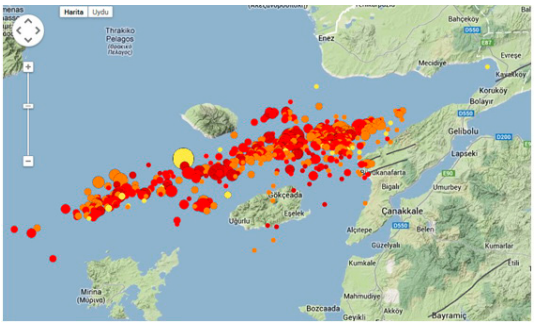

Figure 4. The aftershock distribution of events between May 24th and 30th May 2014 (quick solition by KOERI).
Şekil 4. 24-30 Mayıs 2014 tarihleri arası artçı depremlerin dağılımı (KRDAE tatafından yapılmış hızlı çözümler)

One of the prerequisites for such long rupture area is a shallow seismogenic source zone. Indeed, the Aegean crustal structure possesses quite a thin seismogenic crustal thickness manifested by the unusually long duration small amplitude Pn phases observed at the land stations at NW Anatolia followed by large amplitude Pg phases. Even such Pn phases are recorded at short epicental distances being a strong evidance for such a thin crust overlaying the Mantle.

Yet another, distinct characteristic feature associated with the North Aegean Sea Earthquake is the long period seismic waves recorded at the stations deployed in eastern Marmara region. The causatives for such long period waves is a challenge both for the Earthquake Early Warning and Earthquake engineering studies since the long periods waves are effective even at locations several hundreds km away from the source region. The Gökçeada strong motion station located about 50 km to the south of the source zone acquired the long period source pulses associated with the rupture of the fault plane. Considering the strike-slip faulting mechanism of the earthquake and the location of the Gökçeada station the long pulses portrays the fault normal motions acquired because of the fact that the station is located close to the nodal plane for the shear waves (Figure 5).

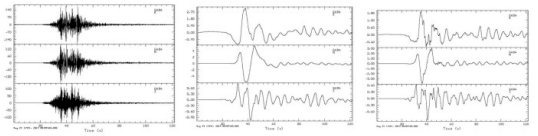

5a 5b

Figure 5. Long period pulses associated with the 2014 North Aegean earthquake recorded at Gökçeada strong motion station. The station is close to the nodal plane of the shear waves (**5a**- Gokceada station acceleration record (from AFAD); **5b**-calculated velocity from acceleration; **5c**-calculated displacement).

Şekil 5. 2014 Kuzey Ege Denizi depreminin Gökçeada ivme-ölçer istasyonunda kaydedilmiş uzun peryot salınımları. İstasyon makaslama dalgası düğüm düzlemine yakın (**5a**- Gökçeada ivme-ölçer kaydı (AFAD), **5b**-ivmeden dönüştürülmüş hız kaydı **5c**- yerdeğiştirmeye dönüştürülmüş kayıt).

TELESEISMIC BODY-WAVE MODELING

One of the most effective tools to infer details on the source rupture process of large earthquakes is modeling of the teleseismic bodywaves. The large aftershock area may reflect the co-seismic rupture zone and the events triggered by the mainshock as a result of Coulomb failure stress changes. To test the hypothess first we obtain a slip distribution model for the mainshock and then using the finite source model we estimate the Coulomb failure stress changes with the aim to understand which part of the aftershock zone are associated as triggered events.

Using the complex teleseismic bodywave records generated by the earthquake and the method developped by Kikuchi and Kanamori (2003) we estimated the seismic moment release on each subfault grid distributed along the strike and dip of the ruptured fault plane (Figure 6).

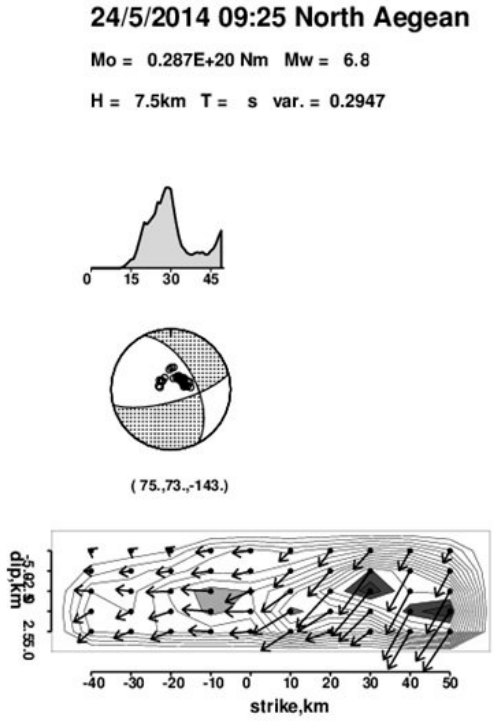

Figure 6. 2D slip distribution along the ruptured fault plane.

Şekil 6. Yırtılmış fay düzlemi boyunca kayma dağılımının 2 boyutlu gösterilimi.

The grid size of 10x5 km was chosen as 10 km along the strike and 5 km along the dip of the fault plane. The inversion results yield a seismic moment of Mo=2.9 x10^{19} Nm (Mw=6.9) and approximately 30 sec source rupture duration. That is consistent with the result of Saltogianni et al., 2015, obtained relatively long source duration (~30 s). The size and arrow of the vectors (rake) shown on the fault plane (Figure 6) characterize the seismic moment tensor derived for each grid point. The rakes illustrated

in Figure 6 suggests that the region to the west of the epicenter experienced mainly strike-slip motion while to the east considerable dip-slip component contrubuted to the motion on the fault plane.

COULOMB FAILURE STRESS CHANGES

The slip distribution model portreyed in Figure 6 was used to estimate the co-seismic static stress changes associated with the mainshock. In our calculations we used a frictional coefficent of 0.3 which is one of the parameters affecting the spatial distribution of the Coulomb stress changes for the optimally oriented fault planes. Considering the predominantly strike slip mechanism for most of the events in North Aegean we used a regional stress tensor appropriate for strike-slip tectonic regimes. The aizmuth of the maximum principle axis was fixed at 290 degree. The results with the fixed parameters are shown in Figure 7. Here, the red colour indicates the areas of increased stress changes and the blue regions show the region were the stress changes are negative.

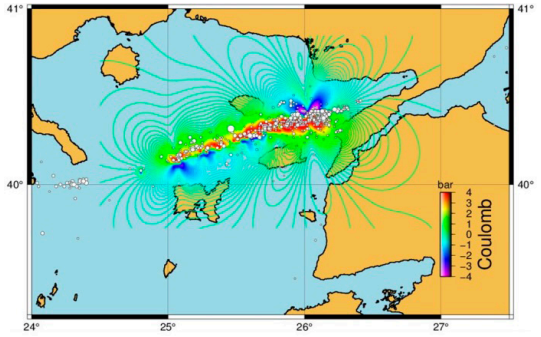

Figure 7. Coulomb stress changes associated with the mainshock.
Şekil 7. Anaşok'un Coulomb gerilim değişimi.

The source rupture process of the North Aegean earthquake is rather important from the view point of understanding whether the increased static stress changes are high enough to trigger the expected large Marmara earthquake. To explore the hypothesis, we constructed an east-west cross-section of the Coulomb stress changes based on the results presented in Figure 7 so as to explore the eastward extension of the stress changes toward the Saros bay (Figure 8).

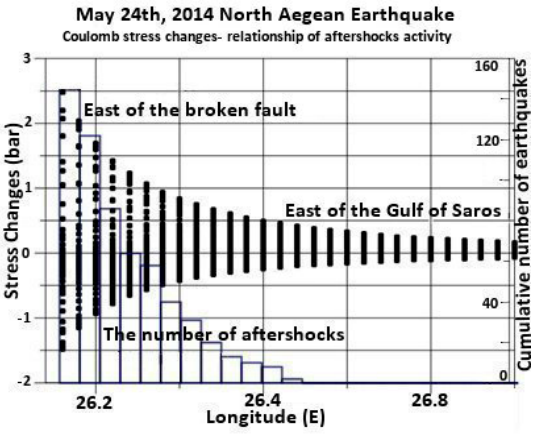

Figure 8. A relation between the number of aftershocks and the stress changes to the east of the ruptured plane. (the black dots are the stresses and the histogram show the number of the aftershocks).
Şekil 8. Yırtılma düzleminin doğusuna doğru artçı deprem sayısı ile gerilme değişimi ilişkisi (siyah noktalar gerilmeleri ve histogram ise artçı depremlerin sayısını göstermektedir).

Such a cross section reveals that the Coulomb stresses exponentially decreases starting from the eastern termination of the rupture toward the east. Besides, it is obvious from Figure 8 that the aftershocks taking to the east of the mainshock area are the events triggered by the static stress increase rather than events taking place on a ruptured fault plane. Most of the aftershocks consantrate at region where the stress incress is between 0.5-3.0 bars. This result has been shown to be consistent with the previous study (Görgün and Görgün, 2015). The region where the stress is less than 0.5 bar the aftershock activity diminishes.

The fault segments to the east of the ruptured area were broken by 1912 Şarköy-Mürefte (Mw=7.4) and the 1975 Saroz bay (Mw=6.3) earthquakes. The surface ruptures on the Ganos fault segment, extending from Saros bay towards Marmara sea, associated with the 1912 earthquakes reveal that the coseismic maximum displacements were in the range between 4 to 5 m (Figure 9; Aksoy et al., 2010; Görgün and Görgün, 2015). This in turn imply that the Ganos fault segment is a strong fault to bear stresses capable to generate 5 m slip.

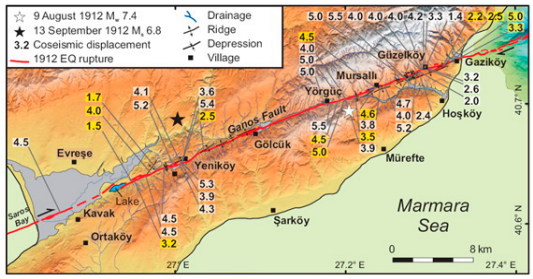

Figure 9. Lateral displacements measured from the surface ruptures associated with the 1912 Şarköy-Mürefte Earthquake (Aksoy et al., 2010).
Şekil 9. 1912 Şarköy-Mürefte depreminin yüzey kırığıyla ilişkilendirilmiş yanal yer değişimler (Aksoy ve diğ., 2010)

On the other hand, the GPS study carried out by Ergintav et al. (2007) shows that the slip rate along the Ganos fault segment is about 17 mm/yr. Thus, the level of strain already accumulated on that fault is far below the maximum bearable stress range of the Ganos segment. Thus, considering all these facts and the stress increases on the Ganos fault caused by the last North Aegean earthquake one may claim that the increased seismic risk is within the range already predicted by the seismic hazard maps.

By virtue of the fact that, the fault segments expected to be ruptured by the impending Marmara earthquake occur further east of the Ganos fault, the coseismic static stress loading caused by the last North Aegean earthquake on those fault segments should be negligible in the order of milibars (Figure 7 and Figure 8).

MOMENT TENSOR INVERSION

In this study we calculated 25 CMT parameters for the strongest events of the 2013 and 25 CMT solutions for the 2014 sequences. We used regionally recorded broad-band velocity waveforms for CMT solutions. We calculated moment tensors of the mainshocks and their strong aftershocks. Moment Tensor Inversion Technique (TDMT_INV time-domain inversion code Dreger, 2002) was used for the earthquakes recorded by at least 4 digital broadband seismic stations of KOERI and other Greek seismological networks with 3-component recordings filtered by a band-pass filters described below. An example for a well-constrained CMT solution is illustrated in Figure 10 and Figure 11. The quality (good signal-to-noise ratio) of the available data allowed the computation of 50 earthquake focal mechanisms and source depths (Table 2). Green's functions were calculated using the frequency-wave number integration code (FKRPROG) developed by Saikia (1994).

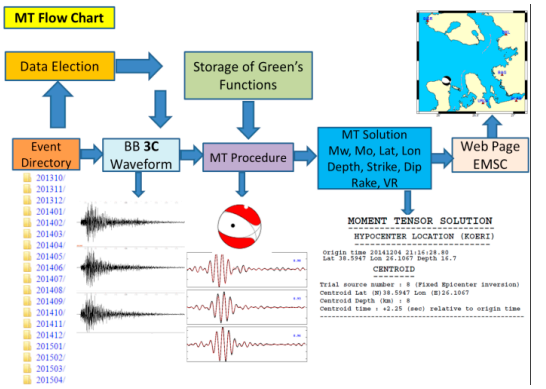

Figure 10. Fault Mechanism /CMT Solution Flowchart (Kalafat et al., 2009).
Şekil 10. Fay mekanizması/ CMT çözüm akış diyagramı (Kalafat ve diğ., 2009).

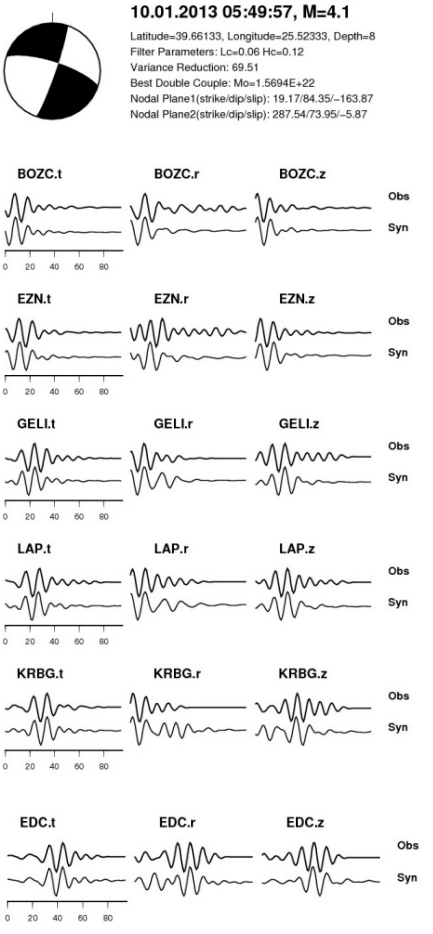

11.01.2013 00:30:19, M=4.5

Latitude=39.681, Longitude=25.50633, Depth=10
Filter Parameters: Lc=0.035 Hc=0.06
Variance Reduction: 61.64
Best Double Couple: Mo=6.0108E+22
Nodal Plane1(strike/dip/slip): 241.23/71.12/–83.99
Nodal Plane2(strike/dip/slip): 43.20/19.78/–107.03

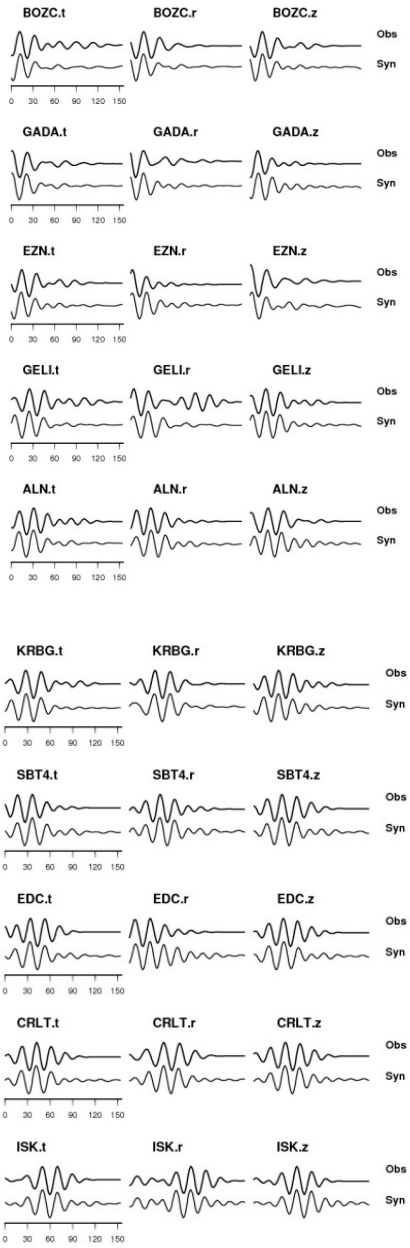

11.01.2013 15:07:30, M=3.8

Latitude=39.68833, Longitude=25.60383, Depth=10
Filter Parameters: Lc=0.05 Hc=0.1
Variance Reduction: 65.54
Best Double Couple: Mo=4.9457E+21
Nodal Plane1(strike/dip/slip): 235.79/67.53/–143.97
Nodal Plane2(strike/dip/slip): 130.26/57.08/–27.08

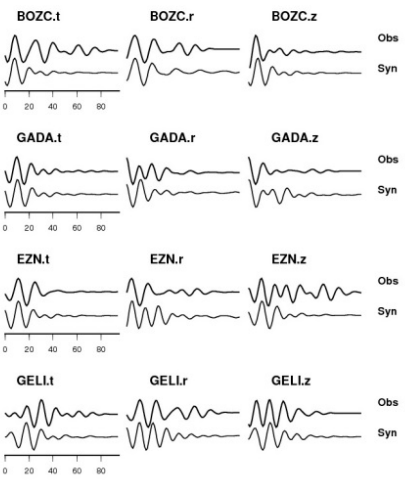

11.01.2013 21:56:16, M=4.1

Latitude=40.40533, Longitude=25.9495, Depth=14
Filter Parameters: Lc=0.05 Hc=0.1
Variance Reduction: 65.08
Best Double Couple: Mo=1.7771E+22
Nodal Plane1(strike/dip/slip): 208.63/82.22/–161.03
Nodal Plane2(strike/dip/slip): 115.96/71.21/–8.22

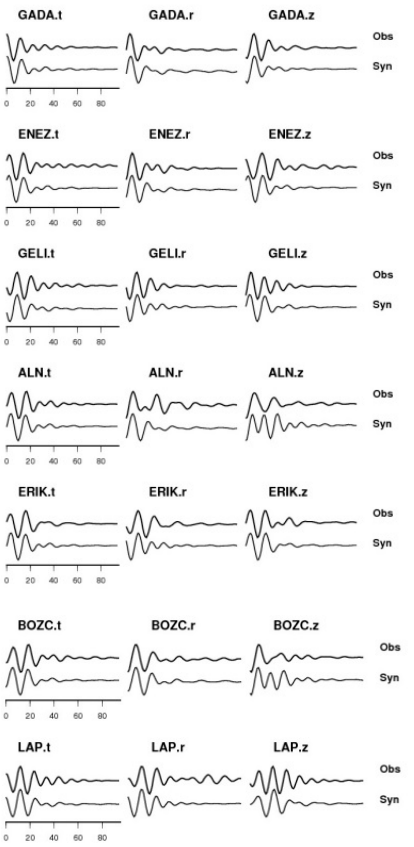

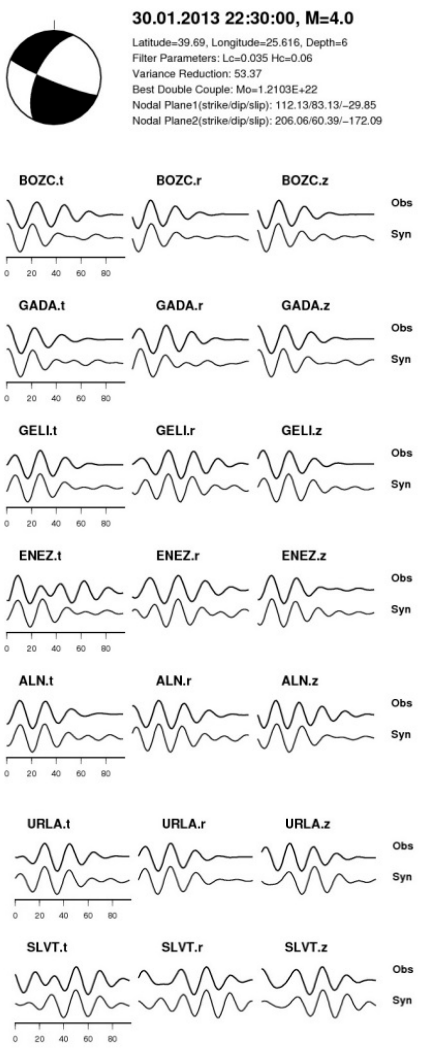

Figure 11. Examples of inversion.
Şekil 11. Ters çözüm örnekleri.

Once we have the the location and magnitude of an event we can proceed on CMT estimation following the two stages given below:

1. Data preparation for inversion
2. CMT Inversion process

In the first stage, the three component digital broadband waveforms are cut according to the origin time, station response is removed, the horizontal components are rotated to get the radial and transversal components, integration or derivation is applied depending on the data type to get the displacements in cm. The modeling process is carried out using the long periods of the seismograms where the frequency range depends on the magnitude of the event. We apply the following frequency ranges for different magnitude ranges:

M<4	0.02 - 0.1	Hz,
4.0≤M<5.0	0.02 - 0.05	Hz,
5.0<M≤7.5	0.01 - 0.05	Hz
M>7.5	0.005 - 0.05	Hz .

The sampling rate of the observed and the calculated seismograms are modified to have the same sampling rate.

STRESS TENSOR INVERSION

The method we use to derive the stress tensor acting on the faults in the North Aegean Sea is described by Gephart (1990) following the same approach we used to derive stress tensor from the focal mechanisms of the events in Marmara region (Pınar et al., 2003) . Our data are the orientation of the P- and T-axes of the fault plane solutions we determined. In the method, the earthquakes are assumed to have occurred in a region with no spatial or temporal changes in the stress field, and the associated slip direction is the shear stress direction on the fault plane. The method yields a stress tensor defined by the three principal stress components, namely, maximum compression, ($\sigma1$), intermediate compression, ($\sigma2$), minimum compression, ($\sigma3$), and the stress magnitude ratio defined as $R = (\sigma2 - \sigma1)/(\sigma3 - \sigma1)$. The value of R is an indicator of the dominant stress regime acting in the region under investigation; $R = 0$ when $\sigma1 \approx \sigma2$ (biaxial deviatoric compression or state of confined extension), $R = 1$ when $\sigma2 \approx \sigma3$ (uniaxial deviatoric compression or state of confined compression) and $R = 0.5$ when $\sigma1 \approx \sigma2 \approx \sigma3$ (uniform triaxial compression). For more information on the subject please refer to Pınar et al. (2003) and the references given therein. The combination of these four parameters ($\sigma1$, $\sigma2$, $\sigma3$ and R) is called a stress model and the model that most closely matches the whole observed data set is called the best-fitting stress model. The best-fitting model is searched for in a grid over the four model parameters, systematically adjusting one at a time through a wide range of possibilities (Gephart 1990). The measure of misfit is given by the smallest rotation about an axis of any orientation that brings one of the nodal planes and its slip direction into an orientation consistent with the stress model.

Thus, for each stress model, the misfits between the orientation of the observed data and prediction are estimated and summed. The minimum misfit is the one that yields the smallest sum of misfits and is selected as the regional stress tensor for the region.

RESULTS

The January 8, 2013 North Aegean Earthquake and its Aftershocks Sequence

The sequence included nine events of magnitude Mw ≥ 4.0 and greater. During the 8 January - 31 March 2014 time period (approximately 2 months) 385 afershocks were relocated in the rupture region. The calculation of epicenters have been done by P and S readings of the seismograms recorded by the Turkish and Greece stations.

In the study, events with at least 5 P- and 1 S-wave arrivals , having azimuthal gap lower than 200, location RMS lower than 0.30 s were chosen for processing. The earthquakes were obtained with horizontal (ERH) and vertical (ERZ) location errors lesser than 2.0 and 1.0 km, respectively. Based on the estimated hypocentral depths, most of the aftershocks occur within the upper crust, within the first 15 km. We relocated 385 events which were well recorded by at least five stations for two month period following the mainshock. Aftershocks are complete for Ml ≥ 2.3 and from the Gutenberg–Richter curve the b-value was calculated to be b =0.703 and the a-value =4.74 (Figure 12).

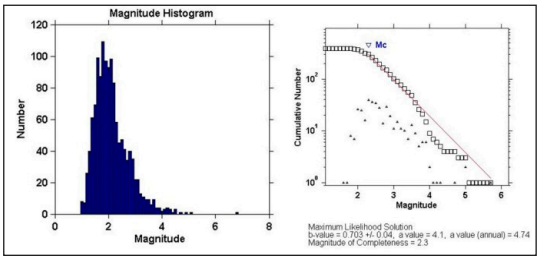

Figure 12. Cumulative number of earthquakes *versus* magnitude (completeness magnitude *Mc*)
Şekil 12. Depremlerin magnitüd kümülatif sayı ilişkisi (Mc magnitüd tamlığı)

8 January 2013 seismic sequence occurred between Lemnos Island, Greece and Bozcaada Island, Turkey in the North Aegean Sea. The distribution of relocated epicentres and the focal mechanisms clearly show the activation of a NE-SW trending right lateral strike-slip fault. This study provided CMT solutions for the mainshock and 24 important aftershocks. The results of this study supports the work done previously which showed that the main shock has a right-lateral faulting mechanism (Kiratzi et al., 2013; Ganas et al., 2013; Kurçer et al., 2014) . The source parameters of the earthquakes are given Table 2 and Figures 13, 14 and the stress tensor inversion results using the focal mechanisms given in Figure 14 is illustrated in Figure 15.

Table 2. January 8, 2013 North Aegean Sea Earthquake Source Parameters (Main Shock+ Big Aftershocks)

Moment Tensor Solutions of the 8 January 2013 North Aegean Sea Earthquake and its important aftershocks
Source Parameters

EQ NUMBER	DATE D/M/Y	TIME UTC	LATITUDE Degrees	LONGITUDE Degrees	DEPTH km	MAGNITUDE Mw	S. MOMENT Nm	FAULT PARAMETERS Strike	Dip	Slip	P axis Azimuth	P axis Plunge	T axis Azimuth	T axis Plunge	REGION
1	08.01.2013	14:16	39.65	25.59	14.0	5.7	4.15E+24	138.7	88.4	-12.8	93.5	10.6	-176.9	7.7	Aegean Sea
2	08.01.2013	14:45	39.63	25.48	6.0	3.8	3.63E+21	144.2	85.6	11.7	278.9	5.5	9.1	11.3	Aegean Sea
3	08.01.2013	15:36	39.65	25.54	6.0	3.8	5.01E+21	215.1	89.7	-135.8	89.3	29.4	-19.3	29.4	Aegean Sea
4	08.01.2013	15:41	39.68	25.67	4.0	4.6	7.82E+22	246.0	89.3	-119.1	129.8	39.1	1.5	37.3	Aegean Sea
5	09.01.2013	15:58	39.70	25.61	10.0	3.6	2.77E+21	78.9	89.8	150.5	128.1	20.7	29.9	20.7	Aegean Sea
6	09.11.2013	17:28	39.70	25.60	10.0	3.5	1.82E+21	24.3	83.0	-159.7	249.3	19.0	156.2	8.5	Aegean Sea
7	10.01.2013	05:49	39.66	25.52	8.0	4.1	1.57E+22	19.2	84.3	-163.9	244.1	15.5	152.2	6.9	Aegean Sea
8	11.01.2013	00:30	39.68	25.61	10.0	4.3	3.69E+22	132.9	76.6	-27.2	88.6	38.2	-176.6	8.8	Aegean Sea
9	11.01.2013	15:07	39.69	25.60	10.0	3.8	4.90E+21	220.6	87.5	-143.9	97.2	40.0	1.2	0.9	Aegean Sea
10	11.01.2013	21:56	40.41	26.56	14.0	4.1	1.76E+23	208.6	82.3	-161.0	73.9	19.0	-18.8	7.4	Gulf of Saros-Aegean Sea
11	12.01.2013	13:47	39.67	25.55	6.0	3.7	4.12E+21	202.5	76.3	-159.6	65.4	23.9	-20.3	3.6	Aegean Sea
12	12.01.2013	16:00	39.65	25.62	8.0	3.6	2.76E+21	119.4	88.7	-12.3	74.3	11.3	166.4	6.6	Aegean Sea
13	12.01.2013	20:50	39.96	26.00	12.0	3.8	5.15E+21	49.0	74.4	-162.2	270.6	23.9	-179.7	0.9	Aegean Sea
14	13.01.2013	08:55	39.68	25.55	12.0	4.4	4.91E+22	66.5	89.2	-160.1	292.5	28.1	164.6	13.9	Aegean Sea
15	13.01.2013	17:54	39.64	25.62	6.0	4.0	1.12E+22	65.8	74.0	-145.2	290.4	35.9	-167.8	11.2	Aegean Sea
16	16.01.2013	03:17	39.71	25.58	10.0	3.9	7.99E+21	242.6	89.1	-140.4	114.2	27.8	9.1	26.2	Aegean Sea
17	19.01.2013	15:19	39.72	25.46	8.0	3.8	6.05E+21	24.1	89.2	129.3	84.9	27.3	329.1	29.2	Aegean Sea
18	19.01.2013	19:28	39.68	25.57	4.0	3.7	3.85E+21	293.3	87.9	-8.8	248.9	7.1	-20.6	4.2	Aegean Sea
19	30.01.2013	22:30	39.69	25.62	6.0	4.0	1.21E+22	112.1	83.1	-29.6	64.9	25.9	162.6	15.4	Aegean Sea
20	10.02.2013	18:10	39.73	25.59	6.0	3.8	6.39E+21	301.5	85.8	-13.4	256.8	12.0	-11.9	6.3	Aegean Sea
21	05.03.2013	09:44	39.69	25.54	8.0	4.1	1.66E+22	248.9	87.4	-113.2	136.6	43.4	-9.5	37.8	Aegean Sea
22	01.04.2013	16:54	38.85	25.98	14.0	3.9	8.16E+21	324.6	79.7	-18.7	280.8	21.2	12.8	8.2	Aegean Sea
23	30.07.2013	05:33	40.30	25.82	15.0	4.9	2.79E+23	150.2	85.8	-9.5	105.2	9.9	-184.9	4.2	Aegean Sea
24	15.11.2013	20:10	39.82	25.61	8.0	3.8	6.16E+21	55.3	82.1	-131.9	287.8	38.2	176.4	24.9	Aegean Sea
25	18.12.2013	21:20	39.83	25.39	8.0	4.0	1.23E+22	309.2	87.9	-15.9	262.4	12.7	-5.4	9.8	Aegean Sea

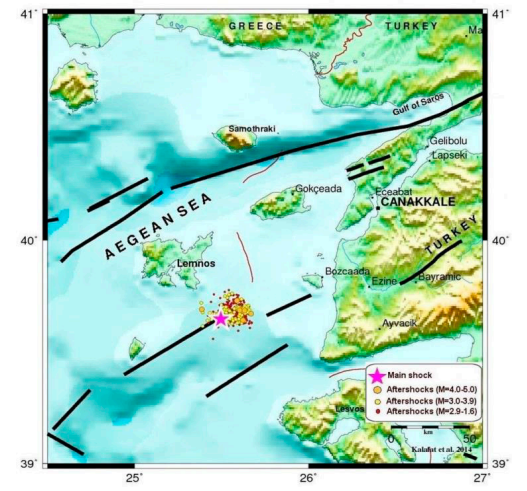

Figure 13. Aftershocks Distribution of 2013 North Aegean Sea Earthquake.
Şekil 13. 2013 Kuzey Ege Denizi depreminin artçılarının dağılımı.

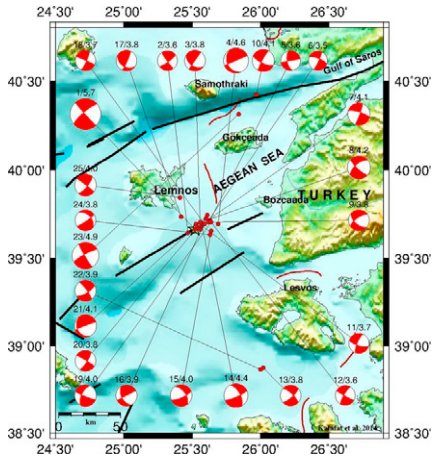

Figure 14. CMT solutions of 2013 North Aegean Sea Earthquakes.
Şekil 14. 2013 Kuzey Ege Denizi depremlerinin faylanma mekanizma çözümleri.

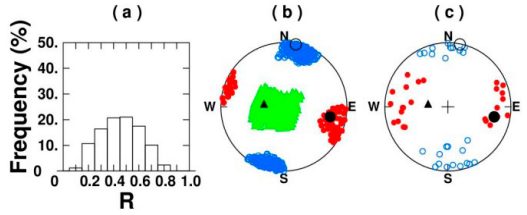

Figure 15. The results of regional stress tensor analysis for the 2013 North Aegean Sea earthquake, based on the P- and T-axes of the focal mechanisms.
(a) the histogram of R-values, (b) the distribution of the predicted principal stress axes and their 95 percent confidence regions and (c) the distribution of the observed P- and T-axes. In (b), red dots show the azimuth and plunge of the maximum stress axis σ1, blue circles those of the minimum stress axis σ3 and green triangles those of the intermediate stress axis σ2. In (c), red dots show the P-axes and blue circles the T-axes. Black symbols denote the axes for the best stress model. For the region, the best fit was attained for R = 0.5 and for the azimuth and plunge pair of (102◦, 26◦) for σ1, (279◦, 64◦) for σ2 and (11◦, 1◦) for σ3, respectively.

Şekil 15. 2013 Kuzey Ege Denizi depremlerinin fay mekanizma çözümlerinin P-T eksenleri dağılımından elde edilmiş bölgesel gerilme tensör analizi sonuçları. (a) R değerlerinin grafiği, (b) ana gerilme eksenlerinin dağılımı ve %95 güvenirlilik bölgeleri ve (c) gözlenmiş P ve T eksenlerinin dağılımı. Şekil b'de kırmızı noktalar σ1 maksimum gerilme ekseninin azimut ve dalımını, mavi daireler σ3 minumum gerilme eksenini ve yeşil üçgenler orta gerilme eksenini gösterir. Şekil c'de kırmızı noktalar P eksenini ve mavi daireler T eksenini gösterir. Siyah semboller en uygun gerilme modelinin eksenlerini gösterir. Çalışma bölgesi için en iyi R = 0.5, azimut ve dalım değerleri σ1 için (102°, 26°), σ2 için (279°, 64°) ve σ3 için (11°, 1°) olarak elde edilmiştir.

The May 24, 2014 North Aegean Earthquake and its Aftershocks Sequence

The second earthquake in this region, 24 May 2014 North Aegean sequence was recorded by the stations of the Turkish and Greek Seismological Networks. In the study, events with at least 7 P- and 1 S-wave arrivals , having azimuthal gap lower than 200, location RMS lower than 0.40 s were chosen for processing. The earthquakes were obtained with horizontal (ERH) and vertical (ERZ) location errors lesser than 2.0 and 1.0 km, respectively. Based on the estimated hypocentral depths, most of the aftershocks occurs within the upper crust, in the first 20 km. 24 May - 31 July 2014 time period (approximately 2 months) 1305 afershocks were relocated in this region. Most of the aftershocks activity took place within the first two months of the earthquake sequence. Aftershocks are complete for Ml ≥ 2.1 and from the Gutenberg–Richter curve the b-value was calculated to be b =0.598 and the a-value =4.03 (Figure 16).

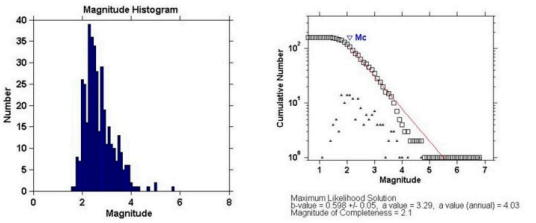

Figure 16. Cumulative number of earthquakes *versus* magnitude (completeness magnitude, *Mc*).
Şekil 16. Depremlerin magnitüd kümülatif sayı ilişkisi (Mc magnitüd tamlığı).

24 May 2014 earthquake occurred also in the North Aegean Sea. The earthquake was felt very strongly in the North Aegean Sea area between Greece and Turkey (Io=VIII, MM). About 300 houses were damaged in Turkey (Figure 17), 11 houses collapsed in Greece and totally 350 people injured in the earthquake.

Figure 17. Some examples of heavily damaged house from Gökçeada Island and Çanakkale (Turkey; by AA).
Şekil 17. Gökçeada ve Çanakkale'de ağır hasarlı binalardan bazı örnekler (Anadolu Ajansı,Türkiye)

The aftershocks continued about 2 months in this area. Along strike dimension of the aftershock zone is approximately ~120 km long, and its width is ~10 km, in accordance to what is expected from the magnitude of the largest event of the sequence (Mw=6.8) assuming 50 cm avarage displacement

(Figure 18). The aftershock zone of the 2014 earthquake was defined a distance of 180-250 km long by Saltogianni et al., 2015. Most of the aftershock focal mechanisms show right-lateral strike-slip faulting (Figure 19; Table 3), as is the case of the mainshock (No. 1). After the mainshock the seismic activity in NW Turkey considerably increased (Figure 20).

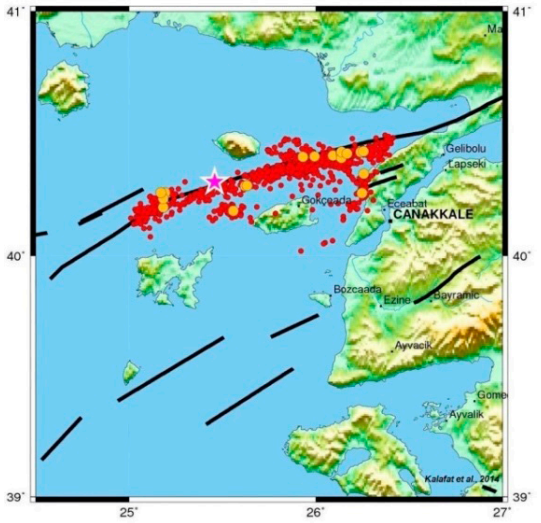

Figure 18. Aftershocks Distribution of 2014 North Aegean Sea Earthquake.
Şekil 18. 2014 Kuzey Ege Denizi depreminin artçılarının dağılımı

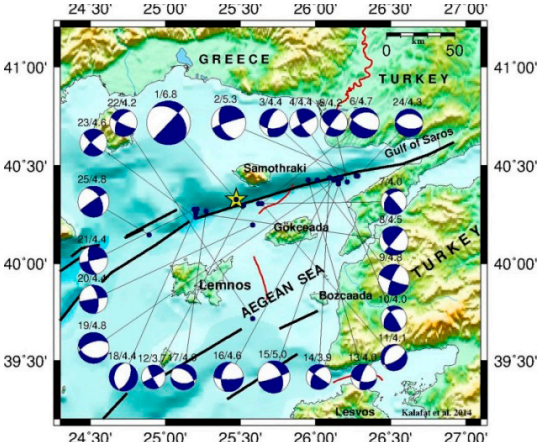

Figure 19. CMT solutions of 2014 North Aegean Sea Earthquakes.
Şekil 19. 2014 Kuzey Ege depremlerinin CMT çözümleri

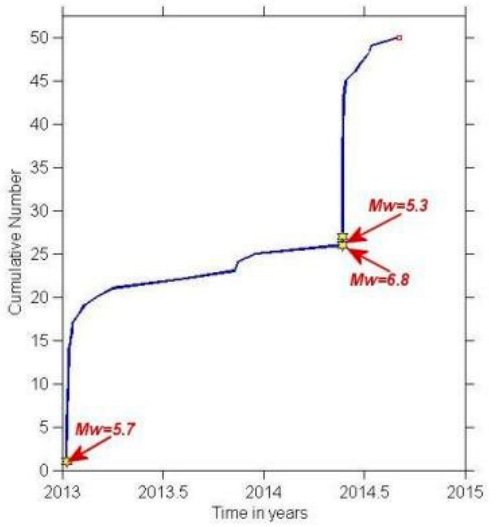

Figure 20. Cumulative distribution of January 8, 2013 and May 24, 2014 North Aegean Sea earthquakes in the region.
Şekil 20. 8 Ocak 2013 ve 24 Mayıs 2014 Kuzey Ege Denizi depremlerinin kümülatif dağılımı.

Based on the distribution of the aftershocks and the focal mechanisms, the **ENE–WSW** trending planes are the fault planes. Also, similar results have been found by Görgün and Görgün, 2015.

Stress Tensor Analysis (STA) was done within the study area for understanding the tectonic properties. The stress tensor parameters are calculated using the azimuth and dip of P and T axis couples of 50 earthquakes (Figure 21) occuring in the aftershock region and the Stress Tensor Inversion software developed by Gephart (1990).

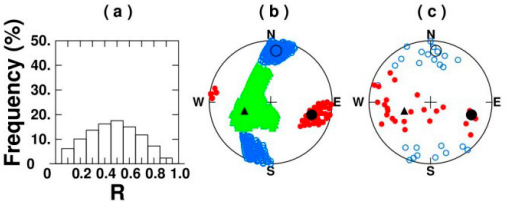

Figure 21. The results of regional stress tensor analysis for the 2014 North Aegean Sea earthquakes, based on the P- and T-axes of the focal mechanisms. For the region, the best fit was attained for R = 0.5 and for the azimuth and plunge pair of (107◦, 31◦) for σ1, (252◦, 53◦) for σ2 and (6◦, 17◦) for σ3, respectively. For more explanation see the caption for Figure 15.
Şekil 21. 2014 Kuzey Ege Denizi depremleri fay mekanizmalarından elde edilmiş P-T eksenleri ve bölgesel gerilme analiz sonuçları. Bölge için en iyi R = 0.5, azimut ve dalım değerleri σ1 için (107°, 31°), σ2 için (252°, 53°) ve σ3 için (6°, 17°) olarak elde edilmiştir. Daha detaylı bilgiyi Şekil 15'in başlığında görebilirsiniz.

The most prominent feature of the earthquake is the widespread distribution of the aftershocks. Whether with, all aftershocks took place along the 120 km length, rupture lenght was a few times shorter than the rupture derived from the aftershok distribution. 2014 North Aegean Earthquake showed that, the long period seismic waves recorded at the stations deployed in eastern Marmara region. The causatives for such long period waves is a challenge both for the Earthquake Early Warning and Earthquake engineering studies since the long periods waves are effective even at locations several hundreds km away from the source region. The Gökçeada strong motion station located about 50 km to the south of the source zone acquired the long period source pulses associated with the rupture of the fault plane. Considering the strike-slip faulting mechanism of the earthquake and the location of the Gökçeada station the long pulses portrays the fault normal motions acquired because of the fact that the station is located close to the nodal plane for the shear waves.

On the other hand, One of the most effective tools to infer details on the source rupture process of large earthquakes is modeling of the teleseismic bodywaves. We obtain a slip distribution model for the mainshock and then using the finite source model we estimate the Coulomb failure stress changes with the aim to understand which part of the aftershock zone are associated as triggered events. Coulomb stress changes associated with the mainshock. The aftershocks tend to take place at regions of increased stress. The southward extension of the aftershock area and the area of increased stress to the east of the epicenter where dip-slip component was derived.

The source rupture process of the North Aegean earthquake is rather important from the view point of understanding whether the increased static stress changes are high enough to trigger the expected large Marmara earthquake. Coulomb stresses exponentially decreases starting from the eastern termination of the rupture toward the east. Most of the aftershocks consantrate at region where the stress incress is between 0.5-3.0 bars.

DISCUSSION

The source regions of the North Aegean earthquakes are influenced by both the Aegean extensional regime and the strike-slip regime in the western part of the North Anatolian Fault Zone. Strike-slip faulting changes to oblique-slip faulting, with significant component of extension, as one goes from the Aegean to the coastal area of Western Turkey. Evidence from the distribution of large earthquakes, and geodetic measurements suggests that the active faulting in mainland Greece and the North Aegean Sea is concentrated into a small number of discrete, linear zones that bound relatively rigid blocks (Goldsworthy et al., 2002).

The prevailing N-S extension in the whole back arc Aegean region is then the key motion that results in dextral strike-slip movement on NE-SW trending faults and sinistral strike-slip movement on NW-SE trending faults. This interpretation relies on the assumption that the faults occupying the western Aegean coast are orthogonal to the NE-SW dextral strike-slip faults and mark the boundary between them and E-W normal faults in the mainland of Greece and Western Turkey (Genç et al., 2001; Koukouvelas and Aydin, 2002; Karakostas et al., 2003; Yaltırak, 2012;Chatzipetros et al., 2013; Görgün and Görgün 2015).

The 2013 and 2014 North Aegean Sea Earthquakes caused a regional stress change and triggrred earthquakes on nearby active fault segments in the region. For this reason, seismicity increased very abruptly in the region (Figure 20).

The rupture of the main fault oriented west to east direction caused stress increase and triggered related seismic activity in the North Aegean Sea region. Therefore high seismic activity is observed at northeast-southwest oriented directions of the main NE-SW trending fault which was broken during the 24th May 2014 Earthquake.

Also according to Görgün and Görgün 2015, the May 24 th, 2014 Earthquake clearly indicated that active NE–SW trending right-lateral strike–slip faulting systems are wide-spread in the Aegean region.

The distribution of the aftershocks of the 2014 earthquake support the presence of a rupture of approximately 120±10 km. Aftershocks occurred within an area of approximately 1200 km^2 (Figure 18). The a and b-values for these sequences were estimated to be equal to 4.03 -4.74 and 0.598-0.703, respectively with 90% goodness of fit level. The b-value is lower than the global mean value of 1.0, which indicates that the North Aegean sequence consists of larger magnitude aftershocks and high differential crustal stress in the regime (Wiemer and Katsumata, 1999; Wiemer and Wyss, 2002).

We have obtained local stress tensors for the source regions of the 2013 and 2014 earthquakes and a regional stress tensor for North Aegean Sea region by combining the all focal mechanisms (Figures 15, 21 and 22). The local stress tensor acting in the source region of the 2013 mainshock and the regional stress tensor exibits maximum compressive stress axis and minimum compressive stress axis close to horizontal implying pure strike-slip tectonic regime (Figure 9). Same result given by Görgün and Görgün, 2015. According to their study, the stress tensor inversion results indicate a predominant strike–slip stress regime with a NW–SE oriented maximum principal compressive stress (σ1).

However, the events in the source region of the 2014 event yield stress tensor inversion results where significant deviation of the intermediate stress axis from the vertical and bias of the minimum compressive stress axis from horizintal suggesting transtential tectonic regime. The local stress tensor derived from the 2013 events is close to the parameters of the regional stress tensor suggesting no stress perturbation caused by the 2013 Mw=5.8 mainshock.

The orientation of the maximum compressive stress axis estimated for the three stress tensors is ESE-WNW and the orientation of the minimum compressive stress axis is NNE-SSW. The plunge of both the axes is close to horizontal. Comparing these stress tensor inversion results with the ones obtained using the events located further east along the North Anatolian fault in Marmara Sea region (Kiratzi 2002 and Pınar et al., 2003) point out significant counterclockwise rotation of the stress field going from east to west.

CONCLUSIONS

The focal mechanism solutions of the important aftershocks of the North Aegean Sea earthquakes show the region is undertaking deformation where right-lateral strike-slip and oblique normal faulting occur (Figure 14, 19).

The distribution of the important earthquakes and aftershocks also provided that E-W and NE-SW trending faults caused the seismic activity in the region (Figure 13, 18). 2013 and 2014 North Aegean earthquakes are good example of the right-lateral fault zones terminate in well-defined extensional basins. The focal depth solutions show that the seismogenic zone producing earthquakes is in 8-15 km depth range which is not very deep.

Likewise, this result is supported by earlier studies. The thickness of brittle seismogenic crust in NAT area is about 25 km (Güngör and Güngör, 2015; Karabulut et al, 2006).

The results of the stress analysis show that the (**P**-compressional) direction of the stress axes is in **WNW-ESE** direction and (**Tmax**-extensional) direction is in **NNE-SSW** direction (Figure 22).

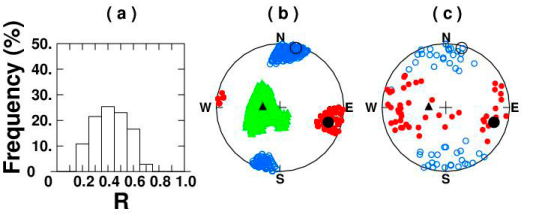

Figure 22. The results of regional stress tensor analysis for the 2013 and 2014 North Aegean Sea earthquakes, based on the all the P- and T-axes of the focal mechanisms. For the combined region, the best fit was attained for R = 0.4 and for the azimuth and plunge pair of (107◦, 22◦) for σ1, (275◦, 68◦) for σ2 and (15◦, 4◦) for σ3, respectively.

Şekil 22. 2013 ve 2014 Kuzey Ege Denizi depremlerinin fay mekanizmalarından elde edilmiş P-T eksenlerinden bölgesel gerilme analiz sonuçları. Bölge geneli için en iyi R = 0.4, azimut ve dalım değerleri σ1 için (107◦, 22◦), σ2 için (275◦, 68◦) ve σ3 için (15◦, 4◦) olarak elde edilmiştir.

The stress field along the North Anatolian fault zone in NW Turkey and North Aegean Sea region rotates counterclockwise moving from east to west.

Coulomb stress changes associated with the mainshock. The aftershocks tend to take place at regions of increased stress. The southward extension of the aftershock area and the area of increased stress to the east of the epicenter where dip-slip component was derived.

One of the characteristics of the North Aegean Earthquake has been shown large amplitude seismic waves. The causatives for such long period waves is a challenge both for the Earthquake Early Warning and Earthquake engineering studies since the long periods waves are effective even at locations several hundreds km away from the source region.

According to the GPS study, the slip rate along the Ganos fault segment is about 17 mm/yr (Ergintav et al., 2007). Thus, the level of strain already accumulated on that fault is far below the maximum bearable stress range of the Ganos segment. Thus, considering all these facts and the stress increases on the Ganos fault caused by the last North Aegean earthquake one may claim that the increased seismic risk is within the range already predicted by the seismic hazard maps.

ÖZET

Bu çalışmada 2013 ve 2014 yıllarında Kuzey Ege Denizinde meydana gelen deprem etkinlikleri incelenmiştir. 17 ay aralıkla bölgede meydana gelen Mw=5.7 ve Mw=6.8 büyüklüğündeki 2 farklı deprem ve bunların artçılarının dış merkez çözümleri yeniden yapılmıştır. Ayrıca meydana gelen önemli büyüklükteki depremlerin (genelde M≥4.0) moment tensör analizleri yapılarak, depremlerin ne tür bir faylanma ile meydana geldiğini, bölgedeki gerilme değişimi ve gerilme artışının hangi yönde olduğu, meydana gelen depremlerin bölgede mevcut tektonik yapılar ile ilgili ilişkisi araştırılmıştır. Sonuçta, yapılan kaynak parametresi çözümleri Kuzey Ege depremlerinin genel olarak sağ yanal doğrultu atımlı faylanma ile meydana geldiğini, bununla birlikte oblik faylanmaların da bölgede devam eden aktif deformasyon sürecinde etkili olduğunu, gerilme analizi sonuçları da, bölgedeki hakim P_{max}-sıkışma ekseninin **BKB-DGD** yönünde ve T_{max}-genişleme ekseninin de **KKD-GGB** yönünde olduğunu göstermiştir.

ACKNOWLEDGEMENTS

This study was supported by Bogazici University Research Projects Commission under SRP/BAP project No. 6040 and MarDIM SATREPS project. The first author was also supported by the Department of Science Fellowship and Grant programs (2014-2219) of TUBITAK (The Scientific and Technological Research Council of Turkey).

Also, We would like to thank Timur Ustaömer (Editör-in Chief), Mustafa Kemal Tuncer (Associate Editör), first reviewer Ethem Görgün and anonymous reviewer for their constructive comments and suggestions which improved the manuscript.

REFERENCES

Aksoy, M.E., M. Meghraoui, M. Vallée, Z. Çakır, 2010. Rupture characteristics of the A.D. 1912 Mürefte (Ganos) earthquake segment of the North Anatolian fault (western Turkey), Geology, 1v. 38 no. 11 p. 991-994.

Allen, C.R., 1969. Active faulting in northern Turkey,Contr. No. 1577, Div. Geol. Sci. Calf. Inst. Techn.,32.

Barka, A. A., 1992. The North Anatolian Fault zone. Annales Tectonicae, 6, 164–195.

Barka, A. A., Toksöz, M.N., Gülen, L., Kadinsky- Cade, K., 1987. Kuzey Anadolu Fayının Doğu Kesiminin Segmentasyonu, Sismisitesi ve Deprem Potansiyeli, Yerbilimleri, C.14, s.337-352.

Barka, A., and Gülen, L., 1988. New constrains on age and total offset on the North Anatolian Fault Zone: Implications for tectonics of the Estern Mediterranean Region. METU Journal of Pure and Applied Sciences, 21, 39–63.

Chatzipetros A, A. Kiratzi, S. Sboras, N. Zouros, S. Pavlides, 2013. Active faulting in the north- eastern Aegean Sea Islands, Tectonophysics 597–598:106–122.

Drakopoulos J. C. and A. C. Ekonomides, 1972. Aftershocks of February 19, 1968 Earthquake in Northern Aegean Sea and Related Problems, pure and applied geophysics, Volume 95, Issue 1,100-115.

Dreger, D., 2002. Manual of the Time-Domain Momet Tensor Inverse Code (TDMT_INVC), Release 1.1, Berkeley Seismology Laboratory, pp. 18

Dewey, J. F., 1976. Seismicity of Northern Anatolia", Bull. Seis. Soc. Am., 3, 843-868.

Dewey, J. F., & Şengör, A. M. C., 1979. Aegean and surrounding regions: Complex multiplate and continuum tectonics in a convergent zone. Geological Society of America Bulletin, 90,84–92.10.1130/0016-7606.

Ergintav, S., U. Doğan, C. Gerstenecker, R. Çakmak, A. Belgen, H. Demirel, C. Aydın, R. Reilinger, 2007. A snapshot (2003–2005) of the 3D postseismic deformation for the 1999, *M*w=7.4 İzmit Earthquake in theMarmara Region, Turkey, by first results of joint gravity and GPS monitoring, Journal of Geodynamics. 2007 44(1):1-18.

Eyidoğan, H., U. Güçlü, Z. Utku, E. Değirmenci, 1991. Türkiye Büyük Depremleri Makro -Sismik Rehberi (1900-1988), İTÜ Maden Fak. Jeofizik Müh. Böl., İstanbul.

Ganas, A., Z. Roumelioti, V. Karastathis, K. Chousianitis, A. Moshou, E.Mouzakiotis, 2014. The Lemnos January 2013 (Mw=5.7) earthquake: fault slip, aftershock properties and static stress transfer modeling in the north Aegean Sea, J. Seismol (2014) 18:433–455.

Gephart, J.W., 1990. FMSI: A FORTRAN program for inverting fault/slickenside and earthquake focal mechanism data to obtain the regional stress tensor, Com.Geosci., 16, 953-989.

Genç, C.Ş., Ş. Altunkaynak, Z. Karacık, M. Yazman, and Y. Yılmaz, 2001. The Çubukludağ graben, south of İzmir: its tectonic significance in the Neogene geological evolution of the western Anatolia, Geodin. Acta 14, 1-3, 45-55.

Goldsworthy, M., J. Jackson, and J. Haines, 2002. The continuity of active fault systems in Greece, Geophys. J. Int. 148, 596–618.

Görgün, E, B. Görgün 2015. Seismicity of the 24 May 2014 Mw 7.0 Aegean Sea earthquake sequence along the North Aegean Trough, Journal of Asian Earth Sciences 111 (2015) 459–469.

Jackson, J., McKenzie, D.P., 1984. Active tectonics of the Alpine-Himalayan Belt between Western Turkey and Pakistan, Geophys. J. R. Astr. Soc., 77, 185-246.

Kalafat, D., C. Gürbüz, S.B.Üçer, 1987. Batı Türkiye'de Kabuk ve Üst Manto Yapısının Araştırılması, Deprem Araştırma Bülteni, Sayı 59, 43-64 (in Turkish).

Kalafat, D., K. Kekovalı, Y. Güneş, M. Yılmazer, M. Kara, P. Deniz, M. Berberoğlu, 2009. Türkiye ve Çevresi Faylanma-Kaynak Parametreleri (MT) Kataloğu (1938-2008): A Cataloque of Source Parameters of Moderate and Strong Earthquakes for Turkey and its Surrounding Area (1938-2008), Boğaziçi University Publication No=1026, 43p., Bebek-İstanbul.

Karakostas, V.G., E. E. Papadimitriou, G. F. Karakaisis, C. B. Papazachos, E. M. Scordilis, G.Vargemezis, and E. Aidona, 2003. The 2001 Skyros, Northern Aegean, Greece, earthquake sequence: off - fault aftershocks, tectonic implications, and seismicity triggering, Geophysical Research Letters, Vol. 30, NO. 1, 1012, doi:10.1029/2002GL015814.

Kalafat, D. Y. Güneş, K. Kekovalı, M. Kara, P. Deniz, M. Yılmazer, 2011. Bütünleştirilmiş Homojen Deprem Kataloğu (1900-2010; M ≥4.0) A revised and extended earthquake cataloque for Turkey since 1900 (1900-2010; M ≥4.0), Boğaziçi University Library Cataloging-in Publication Data, 640p., İstanbul.

Kreemer, C., N. Chamot-Rooke, and X. Le Pichon (2004). Constraints on the evolution and vertical coherency of deformation in the Northern Aegean from a comparison of geodetic, geologic and seismologic data, Earth Planet. Sci. Lett., 225(3–4), 329–346, doi:10.1016/j.epsl.2004.06.018.

Koukouvelas, I., Aydin, A., 2002. Fault structure and related basins of the North Aegean Sea and its surroundings. Tectonics 21 (5). http://dx.doi.org/10.1029/2001TC

Kiratzi A.A., 2002. Stress tensor inversions along the westernmost North Anatolian Fault Zone and its continuation into the North Aegean Sea, Geophys. J. Int., 151, 360-376.

Kiratzi AA, Svigkas, N., 2013. A study of the 8 January 2013 Mw5.8 earthquake sequence (Lemnos Island, East Aegean Sea), Tectonophysics 608:452–460.

Kikuchi, M. and H. Kanamori, 2003. Note on Teleseismic Body-Wave Inversion Program, http://www.eri.u-tokyo.ac.jp/ETAL/KIKUCHI.

Klein F.W., 2002. User's Guide to HYPOINVERSE–2000, a Fortran Program to Solve for Earthquake Locations and Magnitudes, USGS Open-File Report 02-171.

Kürçer, A., H. Yalçın, L. Gülen, D. Kalafat, 2013. 8 January 2013 Mw=5.7 North Aegean Sea Earthquake and its seismotectonic significance, Geodinamica Acta, DIO:10.1080/09853111.2014.957503, 14p.

Lee, W.H.K., Lahr, J.C., 1975. HYPO71: a computer program for determining hypocenter, magnitude and first motion pattern of local earthquakes. USGS Open File Rep. 75–311, 1– 116.

Le Pichon, X., N. Lybéris, and F. Alvarez (1987). Discussion on the subsidence of the North Aegean Trough: An alternative view, J. Geol. Soc., 144(2), 349–351, doi:10.1144/gsjgs.144.2.0349.

McKenzie, D., 1972. Active tectonics of the Mediterranean region, *Geophys. J. Roy. Astr. Soc.* **30**, 2,109-185, DOI: 10.1111/j.1365-246X.1972.tb02351.x.

McKenzie, D., 1978. Active tectonics of the Alpine–Himalayan belt, the Aegean Sea and surrounding regions. Geophys. J. Roy. Astron. Soc. 55, 217–254.

McKenzie, D., & Jackson, J., 1983. The relationship between strain rates, crustal thickening, paleomagnetism, finite strain and fault movements within a deforming zone. Earth and Planetary Science Letters, 65, 182–202.

McClusky, S., S. Balassanian, A. Barka, C. Demir, S. Ergintav, I. Georgiev, O. Gurkan, M. Hamburger, K. Hurst, H. Kahle, K. Kastens, G. Kekelidze, R. King, V. Kotzev, O. Lenk, S. Mahmoud, A. Mishin, M. Nadariya, A. Ouzounis, D. Paradisis, Y. Peter, M. Prilepin, R. Reilinger, I. Sanli, H. Seeger, A. Tealeb, M.N. Toksöz, and G. Veis, 2000. Global Positioning System constraints on plate kinematics and dynamics in the eastern Mediterranean and Caucasus, J. Geophys. Res. 105, B3, 5695-5719.

Nalbant, S.S, A. Hubert, G.C.P King, 1998. Stress coupling between earthquakes in northwest Turkey and the north Aegean Sea. J. Geophys. Res. 103 (B10): 24469–24486.

Papazachos, C.B., 1999. Seismological and GPS evidence for the Aegean–Anatolia interaction, Geophys. Res. Lett. 26, 17, 2653-2656, DOI: 10.1029/1999GL 900411.

Papazachos, B.C., E.E. Papadimitriou, A.A. Kiratzi, C.B. Papazachos, and E.K. Louvari, 1998. Fault plane solutions in the Aegean Sea and the surrounding area and their tectonic implication, Boll. Geof. Teor. Appl. 39, 3,199-218.

Papadimitriou, E. E., and L. R. Sykes, 2001. Evolution of the stress field in the Northern Aegean Sea (Greece), Geophys. J. Intern., 146, 747–759, 2001.

Papadimitriou E.E, Sykes L.R., 2001, Evolution of the stress field in the northern Aegean Sea (Greece). Geophys J Int. 146(3): 747–759.

Pınar, A, K. Kuge and Y. Honkura, 2003. Moment tensor inversion of recent small to moderate sized earthquakes: implications for seismic hazard and active tectonics beneath the Sea of Marmara, Geophys. J. Int. 153, 133–145.

Reilinger, R., S. McClusky, B. Oral, R. King, M. Toksoz, A. Barka, I. Kinik, O. Lenk, and I. Sanli, 1997. GPS measurements of present-day crustal movements in the ArabiaAfrica-Eurasia Plate collision zone, J. Geophys. Res., 102, 9983-9999, 1997.

Saikia, C., 1994. Modified frequency–wave number algorithm for regional seismo-grams using Filon's quadrature; modelling of Lg waves in eastern North America. Geophys. J. Int. 118, 142–158.

Saltogianni, V, M. Gianniou, T. Taymaz, S. Yolsal- Çevikbilen, S. Stiros, 2015. Fault slip source models for the 2014 *Mw* 6.9 Samothraki- Gökçeada earthquake (North Aegean Trough) combining geodetic and seismological observations; Journal of Geophysical Research: Solid Earth, Volume 120, Issue 12, p. 8610-8622.

Şaroğlu, F., Ö. Emre, E. Herece, 1992. MTA Genel Müdürlüğü web site 1.500 000 scale geological map.

Şengör, A.M.C., Görür, N. and Şaroğlu, F., 1985. Strike-slip deformation, basin formation and sedimentation, Soc. Econ. Paleontologists and Mineralogists, Spc. Publ. 37, 227-264.

Yaltırak, C., E.B. İşler, A.E. Aksu, R.N. Hiscott, 2012. Evolution of the Bababurnu Basin and shelf of the Biga Peninsula: Western extension of the middle strand of the North Anatolian Fault Zone, Northeast Aegean Sea, Turkey, Journal of Asian Earth Sciences 57 (2012), 103–119.

Wells, D.L., Coppersmith, K.J., 1994. New empirical relationships among magnitude, rupture length, rupture width, rupture area, and surface displacement. Bulletin of the Seismological Society of America 84, No. 4, pp. 974–1002.

Wiemer, S., Katsumata, K., 1999. Spatial variability of seismicity parameters in aftershock zones.Journal of Geophysical Research 104, 13135– 13151.

Wiemer, S., Wyss, M., 2002. Spatial and temporal variability of the b-value in seismogenic volumes: an overview. Advances in Geophysics 45, 259–302.

Wessel, P., and W.H.F. Smith, 1998. New, improved version of the Generic Mapping Tools released, EOS Trans. Am. Geophys. Union 79, 47, 579. DOI: 10.1029/98EO00426.

Vannucci, G and P., Gasperini, 2003. The Earthquake Mechanisms of the Mediterranean Area (EMMA); http://www.emsc-csem.org/Earthquake/emma.php.